Tidal stripping of globular clusters in a simulated galaxy cluster

F. Ramos, V. Coenda [1], H. Muriel [1], and M. Abadi [1]
Instituto de Astronomía Teórica y Experimental, CONICET-UNC, Laprida 922, Córdoba, Argentina

ABSTRACT

Using a cosmological N-body numerical simulation of the formation of a galaxy cluster- sized halo, we analyze the temporal evolution of its globular cluster population. We follow the dynamical evolution of 38 galactic dark matter halos orbiting in a galaxy cluster that at redshift $z = 0$ has a virial mass of $1.71 \times 10^{14} M_{\odot} h^{-1}$. In order to mimic both "blue" and "red" populations of globular clusters, for each galactic halo we select two different sets of particles at high redshift ($z \approx 1$), constrained by the condition that, at redshift $z = 0$, their average radial density profiles are similar to the observed profiles. As expected, the general galaxy cluster tidal field removes a significant fraction of the globular cluster populations to feed the intracluster population. On average, halos lost approximately 16% and 29% of their initial red and blue globular cluster populations, respectively. Our results suggest that these fractions strongly depend on the orbital trajectory of the galactic halo, specifically on the number of orbits and on the minimum pericentric distance to the galaxy cluster center that the halo has had. At a given time, these fractions also depend on the current clustercentric distance, just as observations show that the specific frequency of globular clusters S_N depends on their clustercentric distance.

Subject headings: galaxies: clusters: general — galaxies: star clusters: general — methods: numerical

1. Introduction

Galaxy clusters are extreme environments where thousands of galaxies orbit inside a massive system of $\sim 10^{14} M_{\odot}$, a few Mpc size, and with a typical velocity dispersion of $\sim 1000\,\mathrm{km\,s^{-1}}$. In these regions, galaxies evolve under the influence of the strong general tidal field generated by the clusters gravitational potential and also by individual mutual gravitational interactions with other galaxies (e.g. Merritt 1983, 1984; Malumuth & Richstone 1984).

From the theoretical point of view, it is expected that the global tidal field in a massive galaxy cluster will be strong enough to truncate dark matter halos of individual galaxies (Merritt 1983). Diemand, Kuhlen & Madau (2007) found that the removal of the dark matter halo happens from the outside in, i.e. the outer particles of a halo are less bound and thus more prone to be removed. Although the baryonic material is much more concentrated than the dark matter, it can also suffer the effects of the galaxy cluster tidal field. Using N-body/hydrodynamic simulations, Limousin et al. (2009) investigated the effect of tidal stripping on galaxy clusters, tracking both the dark matter halo and the stellar component, and found that the dark matter component is preferentially stripped, while the stellar component is less affected by tidal forces.

Globular cluster systems are among the most extended galactic stellar components; they can reach out well beyond the detectable stellar halo and are also prone to being tidally stripped. Since dark matter density in central regions of galaxy clusters is expected to be higher than in their outskirts, this could result in more compact halos in these central regions (Bullock et al. 2001). A similar effect could be expected for globular clusters, lowering their specific frequency S_N (number per luminosity unit) in the central regions of galaxy clusters compared to the outskirts. Forbes, Brodie & Grillmair (1997) found

[1]Observatorio Astronómico de Córdoba, UNC, Laprida 854, Córdoba, Argentina

evidence of this effect in four galaxies in the central region of the Fornax cluster with a marginal dependence of the specific frequency on the clustercentric distance. Coenda, Muriel & Donzelli (2009) searched for similar evidence using data from the ACS Virgo Cluster Survey on board the Hubble Space Telescope. These authors analyzed the S_N in 13 elliptical galaxies and found that S_N increases as a function of both projected and 3D Virgo clustercentric distance, while the projected number density of background globular clusters decreases. These results are interpreted as direct evidence of tidal stripping of globular clusters due to the gravitational potential of the galaxy cluster. In a similar sense, Alamo-Martínez et al. (2013) studied the globular cluster system in the center of the massive galaxy cluster Abell 1689 and estimated that $80,000$ out of a population of $162,000$ are possibly part of the intracluster medium (see also Webb, Sills & Harris 2013). Evidence of tidal stripping of globular clusters has also been found in less dense environments (see for instance Blom et al. 2014). Hudson et al. (2014) use galaxy halo masses based on weak lensing to compute the ratio between the total mass in globular clusters and the halo mass. They found that this ratio is constant with an intrinsic scatter of 0.2 dex and suggested that some of this scatter is due to differing degrees of tidal stripping of the globular cluster systems between central and satellite galaxies.

In the last two decades or so, growing evidence has been collected of a bimodal color distribution of globular clusters (Gebhardt & Kissler-Patig 1999; Kundu & Whitmore 2001; Brodie & Strader 2006). This is usually interpreted as the consequence of differences in metallicity between two co-existing globular cluster populations: one red and metal-rich $[Fe/H] \sim -0.5$ and one blue and metal-poor $[Fe/H] \sim -1.5$ (Brodie & Strader 2006). Peng et al. (2006) found bimodal color distributions for globular clusters in approximately 100 early-type galaxies of the Virgo galaxy cluster. They found that, on average, red globular clusters account for 15% of the total population in faint ($M_B \sim -15.7$) galaxies and up to 60% in bright ($M_B \sim -21.5$) galaxies. Using the same observational data, Coenda, Muriel & Donzelli (2009) fitted power-laws to the projected number density profiles, finding typical logarithmic slope values of $\alpha = -2.4 \pm 0.2$ and $\alpha = -1.7 \pm 0.1$ for red and blue populations, respectively. Although with a large scatter, other authors (see for example Larsen et al. 2001; Bassino, Richtler & Dirsch 2008; Richtler et al. 2012; D'Abrusco et al. 2014) agree that blue GCs usually show a shallower distribution than that corresponding to red GCs in the whole range of radii. Since the blue population is more extended than the red, it is expected that it will be more prone to be tidally disrupted than the red. Indeed, S_N dependence on clustercentric distance reported by Coenda, Muriel & Donzelli (2009) has been detected only for blue but not for red globular clusters. Kartha et al. (2014) compiled a sample of 40 galaxies and found that the relative fraction of blue to red globular clusters decreases with increasing galaxy environmental density for lenticular galaxies. They propose that the outer blue globular cluster population may be stripped away, giving a lower ratio of blue to red.

From the theoretical point of view, an early work of Muzzio, Martinez & Rabolli (1984) analyzed the swapping of globular clusters in Virgo-like cluster of galaxies using ad-hoc N-body numerical simulations. These authors show that (smaller) galaxies in clusters can lose up to 30% of their globular cluster population, with half of this fraction ending up in the intracluster medium and the other half captured by other (larger) galaxies. Bekki & Yahagi (2006) selected globular cluster particles in cosmological N-body numerical simulations and found that intracluster globular clusters can contribute up to 40% of the total globular cluster population in galaxy clusters of mass 1.0 to $6.5 \times 10^{14} M_{\odot}$. More recently, Smith et al. (2013) studied the impact of harassment on the dynamics of globular clusters in early-type dwarf galaxies of clusters. These authors modeled galaxies that evolved for 2.5 Gyr within a potential field that mimics the effects of harassment in clusters, finding that the dynamical behavior of the globular clusters strongly depends on the fraction of bound dark matter remaining in the galaxy. They conclude that when 85% of the initial dark matter halo mass has been removed, globular clusters begin to be stripped.

Using N-body numerical simulations in the framework of the Λ Cold Dark Matter cosmological model, we explore the tidal removal of globular clusters in a Virgo-like galaxy clusters,

focusing on the differences between red and blue populations. In Section 2 we present the numerical simulation used in this work. In Section 3 we describe the method that we apply in order to select dark matter particles from simulated galactic halos that mimic their globular cluster population. In Section 4 we present the main results about the removal of red and blue globular cluster populations. Finally, in Section 5 we discuss the main results and conclusions.

2. The numerical simulation

We address these issues using a dark matter-only cosmological numerical simulation that follows the formation of a galaxy cluster-sized halo. This simulation was presented in detail by Ludlow et al. (2010) to which we refer the interested reader for further technical details. In brief, a region destined to form a galaxy cluster at redshift $z = 0$ is identified in a larger cosmological box of $100\,\mathrm{Mpc}\,h^{-1}$ comoving on a side. Then, this region is resimulated at a higher resolution using a zoom-in technique (Klypin et al. 2001) while the remainder of the box is resampled at a lower resolution. The high-resolution region has 1.44×10^7 dark matter particles filling an amoeba-shaped volume of $1.39\,\mathrm{Mpc^3h^{-3}}$ at a starting redshift of $z = 19$. The original simulation assumes a Λ Cold Dark Matter cosmology with the following parameters: $H_0 = 73\,\mathrm{km\ s^{-1}Mpc^{-1}}$ (i.e. $h = 0.73$), $\Omega_0 = 0.25$ and $\Omega_\Lambda = 0.75$, Both simulations were performed with the GADGET2 code (Springel et al. 2005). High resolution dark matter particle masses of the resimulation are $5.4 \times 10^7 M_\odot h^{-1}$ and the gravitational softening is $1.5\,\mathrm{Kpc}\,h^{-1}$ comoving. At redshift $z = 0$, the simulated galaxy cluster has a virial radius of $R_{vir} = 1.1\,\mathrm{Mpc}\,h^{-1}$, which corresponds to a virial mass $M_{vir} = 1.71 \times 10^{14} M_\odot\,h^{-1}$. These values are comparable to those estimated for the Virgo Cluster (see Karachentsev & Nasonova 2010). Within the virial radius (i.e. radius where the average mass density is 200 times the critical mass density of the universe) at redshift $z = 0$ there are 3.16×10^6 dark matter particles. This halo corresponds to the halo labeled "h14" in Table 1 of Ludlow et al. (2010) which is isolated and virialized at z=0. In order to select the main cluster-sized halos and their galactic subhalos, we use the SUBFIND algorithm (Springel et al. 2001) which identifies substructures inside friends of friends groups. We run SUBFIND on all 100 snapshots, equally spaced in $\log(a)$, from redshift $z = 19$ to $z = 0$ to follow the dynamical evolution of their globular cluster populations. In Fig. 1 we show the projected spatial distribution of dark matter particles (small gray dots) centered in the simulated galaxy cluster at redshift $z = 0$, where the solid circle shows the system virial radius. Using different colors we highlight dark matter particles selected as nine different globular cluster systems, following the method described in the next section. All the remaining globular cluster systems are depicted as gray dots.

3. The model

3.1. Globular cluster population

Using SUBFIND (Springel et al. 2001) we identified the 158 most massive dark matter halos that at redshift $z = 0$ are located inside the virial radius of the galaxy cluster. At z=0, the less massive halo is resolved by at least 200 particles, which corresponds to $M \sim 1 \times 10^{10} M_\odot h^{-1}$, while the most massive one has about 4000 particles, which corresponds to $M \sim 2 \times 10^{11} M_\odot h^{-1}$. We follow the temporal evolution of each halo, computing its mass, density profile, orbit and accretion time i.e. the time when it enters the galaxy cluster virial radius for the first time. In order to perform reliable statistics, we limited our sample to those halos that, at selection time, were resolved by at least 700 particles. In order to maximize the amount of time that halos are orbiting the galaxy cluster, we exclude from our analysis those halos that have late accretion time ($t > 10\,\mathrm{Gyr}$). We have also excluded 19 halos that at the selection time (or even before) had a near neighbor halo. Our final sample has 38 halos.

In Fig. 2 we show the clustercentric distance as a function of time for these 38 halos (gray lines), highlighting the nine halos also highlighted with the same color-coding in Fig. 1. In order to minimize halos with possible tidal distorsions, we checked each halo during the infall process. We noticed that at accretion time many halos are already distorted by the clusters gravitational potential. However, two snapshots before that, halos show no evidence of such distortion. Consequently, we adopt this time as the snapshot to select globular

clusters. Selection time was, on average, 0.5Gyr before the accretion time (shown as vertical lines in Fig.2). We computed the mass density profile of halos at this time, fitting a NFW profile (Navarro, Frenk & White 1996) expressed as:

$$\rho_{NFW}(r) = \frac{\rho^0_{NFW}}{(r/r_{NFW})(1+r/r_{NFW})^2} \qquad (1)$$

where ρ^0_{NFW} and r_{NFW} are the dark matter halos characteristic density and scale length, respectively. Typical accretion cosmic times range between 4.0 and 9.3 Gyrs with a median of 5.2 Gyrs. Scale lengths range between 7.5 to 87.8 Kpc h^{-1} with a median of 10.5 Kpc h^{-1} while virial masses range between 5.3×10^{10} and $1.7 \times 10^{13} M_\odot h^{-1}$ with median $1.7 \times 10^{11} M_\odot h^{-1}$. In order to build up globular cluster populations of each halo, we selected a subsample of their dark matter particles, using the method outlined by Bullock & Johnston (2005) and Peñarrubia, Navarro & McConnachie (2008). In this method, a subset of particles is chosen to follow a given spatial mass density profile $\rho(r)$ following its corresponding energy distribution function:

$$f(\epsilon) = \frac{1}{8\pi}\Big[\int_0^\epsilon \frac{d^2\rho}{d\psi^2}\frac{d\psi}{\sqrt{\epsilon-\psi}} + \frac{1}{\sqrt{\epsilon}}\Big(\frac{d\rho}{d\psi}\Big)_{\psi=0}\Big] \qquad (2)$$

where ψ is the relative gravitational potential and ϵ is the relative energy (see Binney & Tremaine 1987).

In order to construct blue and red globular cluster populations for each halo at accretion time we generate two analytic Hernquist (1990) density profiles

$$\rho_H(r) = \frac{\rho^0_H}{(r/r_H)(1+r/r_H)^3} \qquad (3)$$

where r_H is the scale length and ρ^0_H is the characteristic density. We scaled $r_H = \gamma r_{NFW}$ adopting $\gamma = 3$ for blue and $\gamma = 0.5$ for red globular cluster populations. With this choice for γ at accretion time, the projected density profiles at redshift $z = 0$ are approximately power laws with slopes similar to those observed for blue and red populations (see Section 1). At accretion time, we apply Equation (2) to the Hernquist (1990) and Navarro, Frenk & White (1996) profiles in order to construct their corresponding energy distributions $f_H(\epsilon)$ and $f_{NFW}(\epsilon)$, respectively.

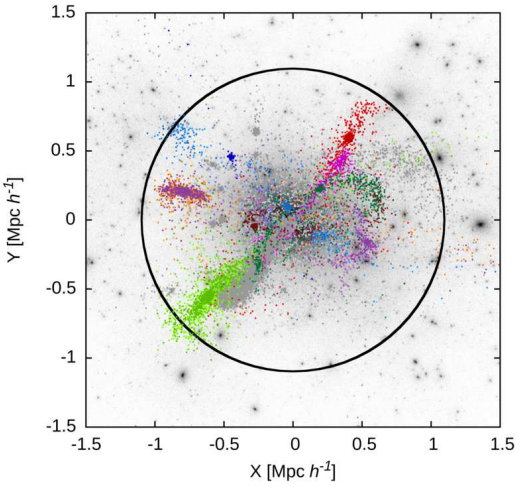

Fig. 1.— Projected spatial distribution of dark matter particles (small gray dots) centered in the simulated galaxy cluster at redshift $z = 0$. The solid circle shows the system virial radius. Different colors show dark matter particles highlighted as blue globular clusters from nine halos, following the method described in Section 3.

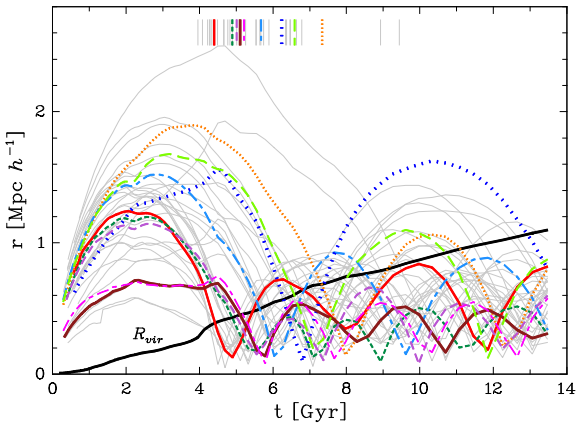

Fig. 2.— Clustercentric distances as a function of time for 38 halos (gray lines). Colors correspond to the nine halos shown in colors in Fig. 1. The black solid line is the virial radius of the cluster. Vertical lines show the time that each halo enters the cluster virial radius.

Then, we randomly select a fraction $f_H(\epsilon)/f_{NFW}(\epsilon)$ of dark matter particles in bins of specific energy $\epsilon + \Delta\epsilon$. Following Bekki & Yahagi (2006) we assume that the baryonic component is more concentrated than the dark matter halo, so we truncate the selection at a cut off radius of $r_{CutOff} = r_{50}/3$, where r_{50} is the half-mass radius of the dark matter halo. As an example, in Fig. 3, we show the projected density profiles $\Sigma(R)$ of one selected halo as a function of the projected distance R, for the dark matter halo (black squares) and for the selected particles chosen to represent the blue (blue circles) and red (red triangles) globular cluster populations. In the *top panel* we show the profile at its accretion time ($t = 4.9\,\mathrm{Gyrs}, \mathrm{z_{in}} = 1.25$) and in the *bottom panel* at the present time ($t = 13.7\,\mathrm{Gyrs}, \mathrm{z} = 0$). This dark matter halo corresponds to that shown in light green in Fig. 1, 2 and 5. The solid black line corresponds to a Navarro, Frenk & White (1996) density profile with concentration $c = 5.9$ and virial mass $M_{vir} = 2.6 \times 10^{12} M_{\odot} h^{-1}$. Blue and red solid lines are not fits to the points, but rather show the analytic Hernquist (1990) profiles chosen to represent both globular cluster populations. Dashed lines show power law fits to the points where we indicate the corresponding slope α for each globular cluster population at accretion time. We follow the temporal evolution of these blue and red populations in order to compare their properties with the corresponding populations observed in galaxy clusters and we present the main results in the next section.

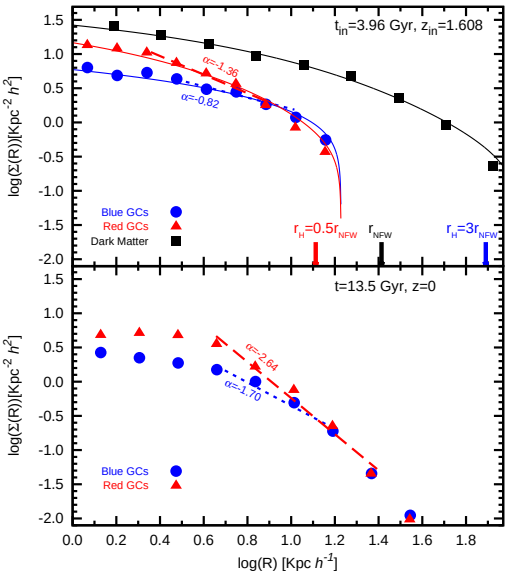

Fig. 3.— Projected radial density profile of one selected halo for dark matter particles (solid black squares), for blue (blue circles) and red (red triangles) globular clusters at redshift z_{in} (*top panel*) in which the halo enters the cluster's virial radius, and at $z = 0$ (*bottom panel*). *Top panel*: The dark halo is modeled as a NFW profile (solid black line), while blue and red globular clusters are modeled as Hernquist profiles (solid blue and red lines, respectively). Vertical arrows show the Hernquist scale length r_H for blue ($3r_{NFW}$) and red ($0.5r_{NFW}$) globular cluster populations, and the NFW scale length (r_{NFW}) for the dark matter halo. In *both panels* we show a power law fit to the data. Short dashed lines correspond to blue globular clusters and long dashed lines to red globular cluster populations.

4. Results

4.1. Density profile of globular clusters

As can be seen in Fig. 4, the density profile of globular clusters is steeper at redshift zero than at the time of selection. We analyzed the evolution of these profiles as a function of redshift and found that the profiles become steeper immediately after the halos enter the cluster. After that, slopes remain nearly constant independently of the evolution of the associated globular clusters. This indicates that, even in those cases where an important fraction of globular clusters is removed, the remaining bound objects are redistributed in order to preserve a certain density profile. This is in agreement with Coenda, Muriel & Donzelli

(2009), who found a lack of dependence between the slopes of the density profiles of globular clusters and the clustercentric distances in the Virgo cluster. Nevertheless, Bekki et al. (2003), using a simple numerical model, found that the radial number density of the globular cluster system becomes steeper after the stripping of globular clusters.

4.2. Globular cluster fraction evolution

In order to follow the temporal evolution of globular clusters orbiting the galaxy cluster, for each halo, we estimate the fraction that is associated with its own main halo at any given redshift. We assume that a globular cluster is associated with its main halo if its distance to the halo center is less than the most distant dark matter halo particle identified by SUBFIND (Springel et al. 2001) as part of this halo. In order to compute this fraction, at any given redshift z, we compute the ratio between the globular cluster number that we have selected at accretion redshift z_{in} and the globular cluster number contained inside a sphere of radius equal to the most distant dark matter particle identified by SUBFIND. Although this selection criterion may result in the inclusion of globular clusters that are not dynamically linked to the halo, this criterion mimics what is usually done with the observational data, where globular clusters are selected up to a given radius. Moreover, we have found that our results are fairly robust if we adopt a binding energy instead of our distance criteria; average differences in the fractions plotted in figures 5, 6, 7 and 8 are always less than 7%.

Fig. 5 shows the fraction of globular clusters associated with its main halo as a function of time for both blue (*top panel*) and red (*bottom panel*) globular clusters (color coding for this figure is the same as that of Fig. 1). The general trend is that at accretion time t_{in} this fraction is, by definition $f(z_{in}) = 1$ and decays to $f(z = 0) \sim 0.6(0.75)$ at redshift $z = 0$ which means that about 40%(25%) of blue(red) globular clusters are removed from its halo to become part of the intracluster population. The steeper slopes in the upper panel of Fig. 5 clearly show that blue globular clusters are more easily removed than red, as expected due to the shallower spatial distribution of the blue population (see Fig. 4). Some temporal oscillations are

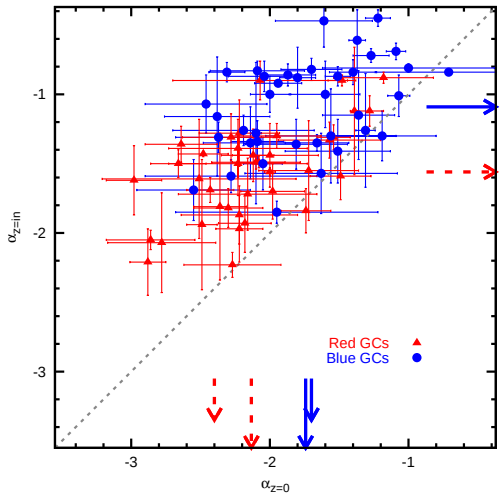

Fig. 4.— Slopes of the projected density profiles of red and blue globular clusters at the redshift z_{in} in which they enter the cluster's virial radius, versus the corresponding slopes at $z = 0$. Symbol and color types as in Fig. 3. Horizontal and long vertical arrows correspond to the median values of slopes for blue (solid blue line) and red (dashed red line) globular cluster populations. Short vertical arrows indicate observed slope values for red and blue CGs. Gray dashed line shows the identity $\alpha_{z_0} = \alpha_{z_{in}}$.

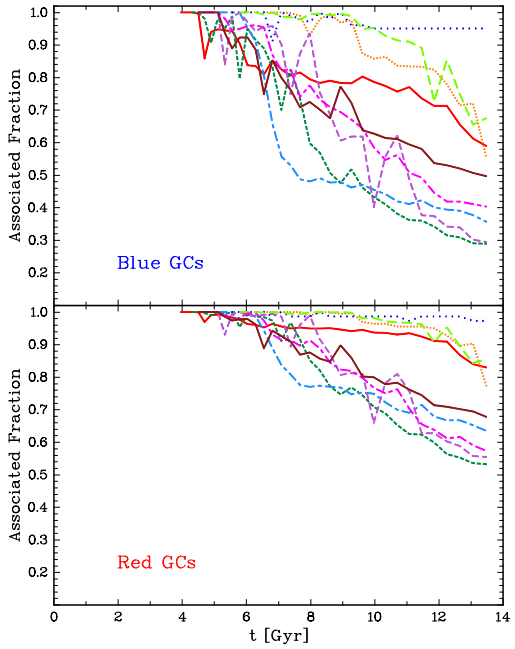

Fig. 5.— Associated fraction of globular clusters as a function of time for blue (*top panel*) and red (*bottom panel*) globular clusters for the same nine halos highlighted in Fig. 1. Color-coding as in Fig.1.

noticeable in the fraction of globular clusters associated with its halo (see for example the purple dashed line). Fig. 2 and 5 show that the local minima correspond to the successive passages of halos through the center of the galaxy cluster. However, it should be noticed that globular clusters are continuously removed throughout the lifetime of halos not only due to pericentric passages. On the other hand, local maxima appear when their orbits intersect a stream of previously removed globular clusters. Also, we followed the fate of the stripped globular clusters and found that none of them are recaptured by other halos.

4.3. Globular cluster fraction and orbital trajectory

The strength of the tidal field generated by the gravitational potential of the galaxy cluster depends on the relative position of halos with respect to the cluster center. Thus, a correlation is expected between the fraction of globular cluster that remains associated with its halo and its orbital parameters. Consequently, we searched for correlations between the fraction of globular clusters associated with its halo and the number of orbital revolutions completed by the halo from accretion time t_{in} to redshift $z = 0$.

In Fig. 6, we plot the fraction of globular clusters at redshift $z = 0$ as a function of the number of orbits; points correspond to median values and vertical error bars are computed using the bootstrap resampling technique. There is a strong anticorrelation between the fraction of globular clusters at redshift $z = 0$ and the number of orbits. At least 30%(25%) of blue(red) globular clusters are stripped when halos have completed three or more orbits, while those that have completed only one orbit lose $\sim 10\%$ of their globular cluster populations. Based on their orbital trajectory, halos will cross the cluster center at different pericentric distances, experiencing tidal forces of different strengths that modify the fraction of globular clusters assigned. Fig. 7 shows the median fraction of globular clusters associated with each halo at $z = 0$ as a function of the minimun pericentric distance that each had throughout its whole temporal evolution. Vertical error bars are computed using the bootstrap resampling technique in bins of pericentric distance containing equal numbers of halos. Those that during their lifetime approached

the cluster core with pericentric distances less than $150\,\mathrm{Kpc}\,h^{-1}$ lose approximately $\sim$40%(25%) of their blue(red) globular cluster population, while halos that remain away from the core with pericentric distances greater than $300\,\mathrm{Kpc}\,h^{-1}$ keep more than $\sim$80%(90%) of their blue(red) population. Both Fig. 6 and 7 reinforce the interpretation that blue globular clusters are more easily removed from halos than red ones due to the different slope of their density profiles. On average, at $z = 0$, halos have lost $\sim 29\%$ of their initial blue globular clusters; this number drops to $\sim 16\%$ for the red population, so it is expected that intracluster globular clusters will be mainly blue.

The fraction of globular clusters that are associated with its halo at redshift $z = 0$ shows a strong correlation with the number of orbits and the pericentric distance; however, none of them are direct observables. In order to compare qualitatively our results with observations, we tested if the fraction of globular clusters associated, at any given redshift, is a function of the clustercentric distance at that particular redshift. Fig. 8 shows the median of the fraction of globular clusters associated with their halo as a function of the clustercentric distance for both red and blue populations. Different line types correspond to different redshift ranges, averaged as indicated by the labels. We can see that associated clusters correlate with the clustercentric distance for three redshift ranges as shown. As expected, the effect depends on redshift, being stronger at redshift zero. Although the fraction of globular clusters that are associated with their halo is not a direct observable, these results can be compared with the findings of Coenda, Muriel & Donzelli (2009) that the specific frequency (S_N) of the blue globular clusters in the Virgo Cluster increases with the clustercentric distance of galaxies.

5. Discussion and conclusions

Using a dark matter-only numerical simulation that follows the formation of a Virgo-like cluster of galaxies, we investigated the role of the cluster tidal field in the evolution of both red and blue globular cluster populations. At redshift $z = 0$, the simulated cluster has a virial mass $M_{vir} = 1.71 \times 10^{14}\,M_\odot\,h^{-1}$, which is comparable to the mass of the Virgo Cluster. We selected 38

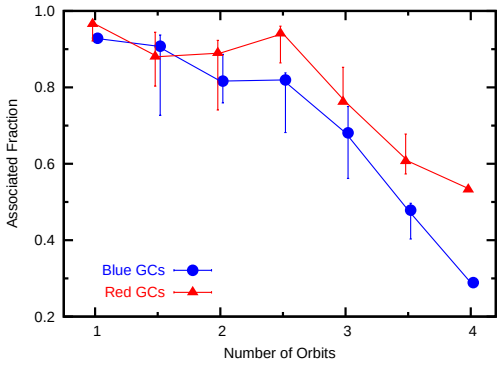

Fig. 6.— Associated fraction of globular clusters as a function of the number of orbits at $z = 0$ for blue and red globular clusters. Points correspond to median values and the vertical error bars are computed using the bootstrap resampling technique. Symbol and color types as in Fig. 3.

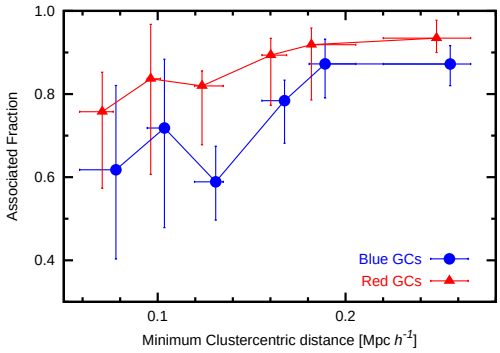

Fig. 7.— Associated fraction of blue globular clusters at $z = 0$ as a function of the minimum clustercentric distance. Points correspond to median values and vertical error bars are obtained using the bootstrap resampling technique. Symbol and color types as in Figure 3.

dark matter halos with $M_{halo} \geq 1.08 \times 10^{10} M_{\odot} h^{-1}$ that entered the cluster virial radius when the Universe was younger than 10 Gyr. Using a Hernsquist profile, we randomly selected globular cluster particles in each dark matter halo, following the method outlined by Bullock & Johnston (2005) and Peñarrubia, Navarro & McConnachie (2008). We used a Monte Carlo procedure to find the parameter that best reproduced the observed density profiles of both red and blue globular clusters. We summarize our principle results as follows.

- Blue globular clusters are lost more easily than red ones. This is an expected result that may be explained by the shallower spatial distribution of blue globular clusters. The stripping of globular clusters is a continuous process that increases with the successive passages of halos through the center of the cluster. On average, halos have lost 16% and 29% of the red and blue globular cluster populations respectively, and therefore a significant number of globular clusters go to the intracluster medium.

- None of the stripped globular clusters are recaptured by other halos.

- Analyzing the bound fraction of globular clusters we found that at least 30% of blue globular clusters are stripped when halos have orbited the cluster of galaxies three or more times. For those halos that have completed only one orbit the fraction removed is $\sim 10\%$.

- We found a strong anticorrelation between the associated globular clusters and the minimum clustercentric distance that the halos have had throughout their history. Halos that have crossed the cluster core within 150 Kpc from the cluster center during their lifetime, lost more than 40% of their blue globular cluster population, while halos that remain away from the core with pericentric distances greater than 300 Kpc, have associated globular clusters greater than 80%.

- The associated globular clusters at a given time correlate with the clustercentric distance. The effect depends on redshift, being stronger at redshift zero. This result is in agreement with observational results (see Coenda, Muriel & Donzelli 2009; Forbes, Brodie & Grillmair 1997).

- The density profile slope of **globular cluster systems** becomes slightly steeper immediately after the halos fall into the galaxy cluster. Thereafter, it remains almost constant, independently of the evolution of the host halo. This result suggests that the density profile of globular clusters remains almost equal over the lifetime of halos, in agreement with the ideas suggested by Coenda, Muriel & Donzelli (2009).

Our results confirm that the stripping of globular clusters produced by the tidal field of clusters of galaxies is an efficient process that may result in significant loss of the original globular cluster population. The magnitude of the effect will depend on the dynamical history of each galaxy. This phenomenon preferentially acts on the blue globular cluster population, and so it is expected that the intracluster globular clusters will be mainly blue.

We thank Aaron Ludlow and Julio Navarro for making these simulations available and for their comments, which improved an earlier version of this paper. We acknowledge Rory Smith, Ken Freeman and Laura V. Sales useful suggestions. We wish to thank the anonymous referee for useful suggestions that have improved the paper. This work has been supported by grants from ANPCYT, CONICET and SECYT-UNC, Argentina.

REFERENCES

Alamo-Martínez K. A. et al., 2013, ApJ, 775, 20

Bassino L. P., Richtler T., Dirsch B., 2008, MNRAS, 386, 1145

Bekki K., Forbes D. A., Beasley M. A., Couch W. J., 2003, MNRAS, 344, 1334

Bekki K., Yahagi H., 2006, MNRAS, 372, 1019

Binney J., Tremaine S., 1987, Galactic dynamics. Princeton, NJ, Princeton University Press, 1987, 747 p.

Blom C., Forbes D. A., Foster C., Romanowsky A. J., Brodie J. P., 2014, MNRAS, 439, 2420

Brodie J. P., Strader J., 2006, ARA&A, 44, 193

Bullock J. S., Johnston K. V., 2005, ApJ, 635, 931

Bullock J. S., Kolatt T. S., Sigad Y., Somerville R. S., Kravtsov A. V., Klypin A. A., Primack J. R., Dekel A., 2001, MNRAS, 321, 559

Coenda V., Muriel H., Donzelli C., 2009, ApJ, 700, 1382

D'Abrusco R., Fabbiano G., Mineo S., Strader J., Fragos T., Kim D.-W., Luo B., Zezas A., 2014, ApJ, 783, 18

Diemand J., Kuhlen M., Madau P., 2007, ApJ, 667, 859

Forbes D. A., Brodie J. P., Grillmair C. J., 1997, AJ, 113, 1652

Gebhardt K., Kissler-Patig M., 1999, AJ, 118, 1526

Hernquist L., 1990, ApJ, 356, 359

Hudson, M. J., Harris, G. L., & Harris, W. E. 2014, ApJ, 787, L5

Karachentsev I. D, Nasonova O. G, 2010, MNRAS, 405, 1075

Kartha S. S., Forbes D. A., Spitler L. R., Romanowsky A. J., Arnold J. A., Brodie J. P., 2014, MNRAS, 437, 273

Klypin A., Kravtsov A. V., Bullock J. S., Primack J. R., 2001, ApJ, 554, 903

Kundu A., Whitmore B. C., 2001, AJ, 121, 2950

Larsen S. S., Brodie J. P., Huchra J. P., Forbes D. A., Grillmair C. J., 2001, AJ, 121, 2974

Limousin M., Sommer-Larsen J., Natarajan P., Milvang-Jensen B., 2009, ApJ, 696, 1771

Ludlow A. D., Navarro J. F., Springel V., Vogelsberger M., Wang J., White S. D. M., Jenkins A., Frenk C. S., 2010, MNRAS, 406, 137

Malumuth E. M., Richstone D. O., 1984, ApJ, 276, 413

Merritt D., 1983, ApJ, 264, 24

Merritt D., 1984, ApJ, 276, 26

Muzzio J. C., Martinez R. E., Rabolli M., 1984, ApJ, 285, 7

Navarro J. F., Frenk C. S., White S. D. M., 1996, ApJ, 462, 563

Peñarrubia J., Navarro J. F., McConnachie A. W., 2008, ApJ, 673, 226

Peng E. W. et al., 2006, ApJ, 639, 95

Richtler T., Bassino L. P., Dirsch B., Kumar B., 2012, A&A, 543, A131

Smith R., Sánchez-Janssen R., Fellhauer M., Puzia T. H., Aguerri J. A. L., Farias J. P., 2013, MNRAS, 429, 1066

Springel V. et al., 2005, Nature, 435, 629

Springel V., White S. D. M., Tormen G., Kauffmann G., 2001, MNRAS, 328, 726

Webb J. J., Sills A., Harris W. E., 2013, ApJ, 779, 94

This 2-column preprint was prepared with the AAS LaTeX macros v5.2.

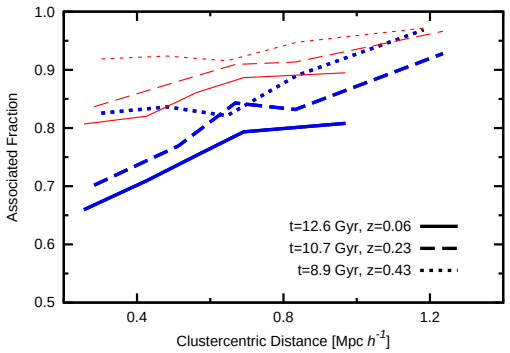

Fig. 8.— Median of the fraction of the blue and red globular clusters associated with its parent halo as a function of the clustercentric distance at different redshifts: $z = 0.06$ (solid line), $z = 0.23$ (long dashed line) and $z = 0.43$ (short dashed lines). Color types as in Fig. 3.